# Tough tri-block copolymer hydrogels with different micro morphologies for medical and sensory materials

*Hui Jie Zhang[1,2], Feng Luo[3,4], Yanan Ye[4,5], Tao Lin Sun[4,6], Takayuki Nonoyama[4,5], Takayuki Kurokawa[4,5], and Tasuku Nakajima*[4,5,7]*

1. Graduate School of Life Science, Hokkaido University, Sapporo 060-0810, Japan

2. College of Bioresources Chemical and Materials Engineering, Shaanxi University of Science and Technology, Xi'an 710021, China

3. College of Polymer Science and Engineering, State Key Laboratory of Polymer Materials Engineering, Sichuan University, Chengdu 610065, China

4. Faculty of Advanced Life Science, Hokkaido University, Sapporo 060-0810, Japan

5. Global Station for Soft Matter, Global Institution for Collaborative Research and Education, Hokkaido University, Sapporo 060-0810, Japan

6. South China Advanced Institute for Soft Matter Science and Technology, South China University of Technology, Guangzhou 510641, China

7. Institute for Chemical Reaction Design and Discovery (WPI-ICReDD), Hokkaido University, Sapporo 001-0020, Japan

*Corresponding author: Dr. Tasuku Nakajima

E-mail: tasuku@sci.hokudai.ac.jp

ABSTRACT

Tough tri-block copolymer hydrogels with microstructures of sphere, cylinder, and laminae were constructed using a newly-developed “drying and swelling” method without changing the chemical structures of their monomeric units. These tough tri-block copolymer hydrogels commonly showed high fracture stress of ~10 MPa but exhibited varied elastic moduli depending on their microstructures. Furthermore, the constructed laminar gel formed pH-sensitive photonic gel at base condition providing the gel application potential as sensor. Given their high toughness, biocompatibility, and tunable modulus, this study helps expand the potential application of amphiphilic block copolymer hydrogels for medical and industrial use.

Keywords: tri-block copolymer, self-assembly, tough hydrogel, sacrificial bond principle, photonic hydrogel

MAIN TEXT

Living tissues contain diverse mesoscale structures with specific structure-related functions or mechanical properties. For example, some bones and nacres form a lamellar structure, which contributes to their high fracture resistance;[1-2] tendons and skin contain aligned collagen fibers to maintain their high mechanical strength.[3] On the other hand, soft and wet hydrogels have gained attention as synthetic substitutes for a variety of living tissues.[4-6] Inspired by the mesoscale structures of living tissues, hydrogels containing various microstructures have been developed to improve their performance. For example, by introducing rigid polymers, hydrogels containing parallel fibrous arrays have been constructed.[7,8] By using amphiphilic lipids[9] or charged nanosheets,[10] hydrogels with a laminar structure were synthesized. However, although each method has realized a specific microstructure with improved material performances, a specially-designed compound is required to produce each specific microstructure in hydrogels. Such chemical restriction for the microstructure construction may lead to unintended chemical properties of the hydrogels, such as cytotoxicity and environmental instability. Establishment of a general method for fabricating a series of hydrogels containing desired but diverse microstructures from the same chemical compounds would be useful for controlling their performances.

Tri-block copolymer (TBC) hydrogels are potential candidates for developing these various microstructures. Block copolymers are well-known for their ability to self-assemble into different microstructures.[11-16] In the case of immiscible binary block

copolymers (AB, ABA, etc.), the microstructures (both bulk and solutions) can be controlled by the volume fraction of each phase.[11-14] Moreover, block copolymers can be synthesized by using various monomers. Thus, in principle, a series of ABA-type TBC gels with different microstructures such as sphere, cylinder, and lamellae can be obtained by controlling the volume fraction of the A-phase without changing the chemical structure of their monomeric units. However, most of the reported microstructures of ABA-type TBC gels are spherical micelles.[17-21] This is mainly because when ABA-type tri-block copolymers are in a B-selective solvent, the B-phase is considered to include not only the B-block chains itself but also the surrounding solvent. As a result, the volume fraction of the B-phase is much larger than that of the A-phase, resulting in formation of a spherical microstructure. For this problem, Shull *et al.* have succeeded to transform microstructure of the ABA tri-block copolymer gels from sphere to cylinder by adding linear A-homopolymers to the TBC gels to increase the volume fraction of the A-block.[22] However, they have not realized the laminar microstructure of the TBC gels. Thus, effect of the microstructure of ABA-type TBC gels, such as sphere, cylinder or lamellae, on their performances has not been fully understood yet.

Thus, this study was conducted to construct ABA-type TBC hydrogels with varied microstructures without altering the chemical structure of their monomeric units. We used poly(butyl methacrylate)-*b*-poly(methacrylic acid)-*b*-poly(butyl methacrylate)

(PBMA-*b*-PMAA-*b*-PBMA) as a model of ABA-type TBCs, where the PBMA A-block was hydrophobic and PMAA B-block was hydrophilic.

Our strategy for construction of multi microstructures in TBC hydrogels is to induce the self-assembly of TBCs through a slow drying-swelling (D-S) process, as shown in Figure 1. Generally, TBC gels are obtained from a homogeneous block copolymer solution by decreasing the solubility of the A-block through temperature control or solvent exchange.[17-19] In these general processes, self-assembly of TBC occurs in the presence of a large amount of B-selective solvent, resulting in the formation of a spherical microstructure. In contrast, we first dissolved the PBMA-*b*-PMAA-*b*-PBMA TBCs in DMF to prepare 20% (w/w) TBC/DMF homogeneous solutions, which were placed in a vacuum drier container containing extra DMF (as shown in Figure 1) for 2 weeks over which the solvent evaporated slowly. During this process, as self-assembly of the TBCs in solution likely occurred in the concentrated state, various microstructures of the TBC were formed by controlling polymerization degree of each block. By completely removing the solvent, the dried TBC sheets, referred to as B(D) sheets, were prepared. Next, the TBC hydrogels, named as B(D-S) gels, were obtained by re-swelling the B(D) sheets in pure water through water absorption by the B-block. During this process, we predicted that the formed hydrophobic microdomains in the B(D) sheets were too energetically stable to dissociate upon swelling. Similar drying-swelling method has been used for construction of the other phase-separated gels[8].

We also intend to toughen the obtained TBC gels by applying the double network principle[23]. Recent approaches have greatly improved the mechanical robustness of TBC hydrogels.[24-26] Particularly, we produced extremely tough semi-interpenetrating polymer network (semi-IPN) hydrogels based on PBMA-*b*-PMAA-*b*-PBMA TBC hydrogels as the first component and linear polyacrylamide (PAAm) as the second component, named as B-DN hydrogels. Because hydrogen bonds formed between the PAAm and PMAA blocks as sacrificial bonds designed to break and dissipate energy under stress, the B-DN hydrogels were extremely tough and strong. Given their excellent mechanical properties, non-cytotoxicity, salt-tolerance, and non-adhesiveness to the tissues, B-DN hydrogels are possible candidates as alternative synthetic materials for replacing living tissues.[25,26]

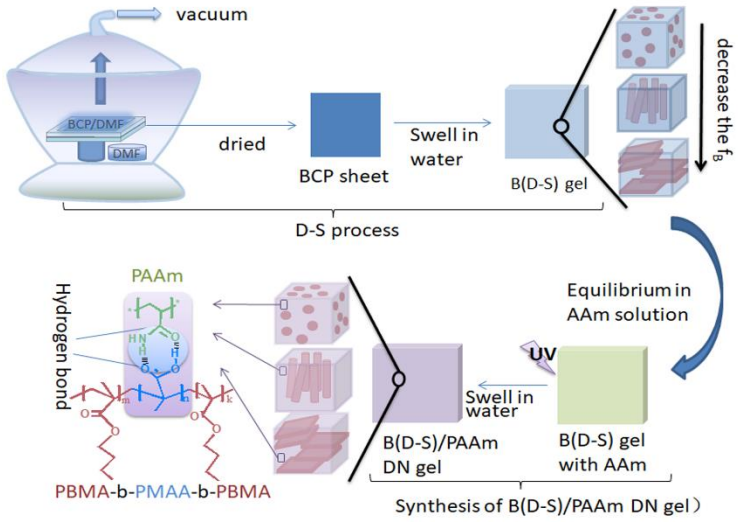


**Figure 1** Scheme of drying-swelling (D-S) process for B(D-S) gel production and scheme for synthesizing the B(D-S)/PAAm gel.

The detailed experimental procedures are shown in the Supporting Information. First, we prepared a series of B(D) sheets and B(D-S) hydrogels as described above from PBMA-*b*-PMAA-*b*-PBMA tri-block copolymers with varying molecular weights of each block and molar fractions of the B-block ($f_B$). A list of the TBCs used is shown in Table S1. As controls, we additionally prepared two types of TBC hydrogels using the fast-drying process (without extra DMF in the vacuum drier container), named as B(FD-S) hydrogels, and using the reported solvent exchange process,[25] named as B(SE) hydrogels. The B(FD-S) hydrogels produced by fast drying were opaque because of inhomogeneous phase separation (as shown in Figure S1). In contrast, the B(D-S) hydrogels obtained by slow drying-swelling were all transparent (as shown in Figure S2b), indicating no macro phase separation and suggesting the importance of slow drying for homogeneous micro phase separation.

Small-angle X-ray scattering (SAXS) measurements revealed that the obtained B(D) sheets and B(D-S) hydrogels had diverse microstructures. As shown in Figure S3, the B(D) sheets and corresponding B(D-S) hydrogels showed similar 1D scattering profiles, suggesting that the microstructure formed in the B(D) sheets did not dissociate after swelling. The 2D and 1D scattering data of the B(D-S) hydrogels are summarized in Figure 2. For the $B_{297}$(D-S) hydrogel (Figure 2a), the 2D SAXS patterns of the top and side views were all isotropic. The peaks in the 1D SAXS profile ($q/q_1$ =1, √2, √3, √4, √5, √6,√8) suggest the cubic packed spherical structure in the hydrogel. At a $q$ value of $q/q_1$ = √3 ,√5, and √6, the scattering peaks were not obvious and covered by the previous peaks, likely because the large size distribution of the ordered structure in the $B_{297}$(D-S) hydrogel caused broadening of the scattering peaks. Thus, the $B_{297}$(D-S) hydrogel was considered to have a typical, cubic packed spherical structure.[13,14] The interdomain space and radius of the A-domain were calculated as 38.7 and 16.1 nm (see Supporting Information for details), respectively.

For the $B_{273}$(D-S) hydrogel, as shown in Figure 2b, the 1D SAXS profile corresponds to reflections of the hexagonally packed cylinder structure ($q/q_1$ =1,√3,√4,√7,√9). The scattering peak at $q/q_1$ = √4 is covered by the previous scattering peak. The interdomain space and radius of the cylinder domain were calculated as 42.7 and 15.5 nm, respectively. The 2D SAXS scattering patterns of the top and side views were all isotropic circles. These indicate that the cylindrical structure in the $B_{273}$(D-S) gel had quite large size distribution and did not arrange in one specific direction.[13,14]

For the $B_{220}$(D-S) hydrogel and $B_{334}$(D-S) hydrogel, as shown in Figure 2c and d, the $q/q_1$ of the scattering peaks in the 1D SAXS profile were 1, 2, and 3, indicating a lamellar structure.[13,14] The laminar spaces and slab thicknesses were calculated as 47.5 and 20.4 nm for the $B_{220}$(D-S) hydrogel and 75.6 and 34.2 nm for the $B_{334}$(D-S) hydrogel, respectively. The 2D SAXS scattering patterns from the top view of the $B_{220}$(D-S) and $B_{334}$(D-S) hydrogels were all isotropic cycles, while from the side view the 2D scattering patterns were anisotropic. The side view pattern of the $B_{220}$(D-S) hydrogel showed a two-point scattering pattern along the thickness direction, indicating a lamellar structure with the layers arranging along the thickness direction. The side view pattern of the $B_{334}$(D-S) hydrogel exhibited ellipse circles, indicating the same arrangement of layers as the $B_{220}$(D-S) hydrogel but a less ordered structure. The lower ordering may be because the higher molecular weight of the $B_{334}$ block copolymer constrained movement of the polymer chains during the D-S process. The structure tendency of these B(D-S) hydrogels obeys that of typical binary tri-block copolymers; the microstructure changed from sphere to cylinder to lamellar structures as the molar fraction of B-block ($f_B$) decreased (Table S2).[11,12]

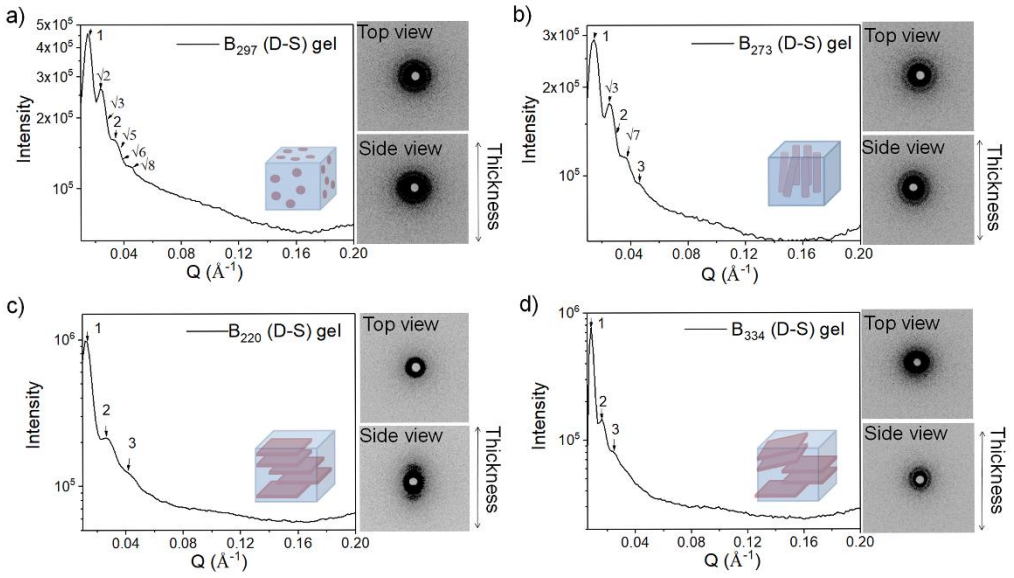


**Figure 2** 1D SAXS profiles of the B (D-S) hydrogels and their 2D SAXS scattering patterns from the top view and side view (on the right side of the 1D profile): a–d) are the SAXS profiles and scattering patterns of the $B_{297}$(D-S) hydrogel, $B_{273}$(D-S) hydrogel, $B_{220}$(D-S) hydrogel, and $B_{334}$(D-S) hydrogel, respectively.

Subsequently, the dependence of the water content and mechanical properties of the B(D-S) gels on their microstructures were studied. The water content of the B(D-S) gels shown in Figure 3a is approximately 30–60 wt%, which is significantly lower than those of the reported TBC gels because of microstructure formation of the TBCs in their dense state[22, 25]. The stress-strain (S-S) curves of B(D-S) gels obtained by the uniaxial tensile test along the length direction are shown in Figure 3b. Notably, some of these hydrogels show high tensile stress of >5 MPa, which is greater than the existing TBC hydrogels.[18, 22, 25] On the other hand, the mechanical response of the B(D-S) hydrogels strongly depends on the used TBCs. When the elastic modulus and work of extension

at the break (toughness) are plotted as a function of $f_B$ (Figure 3c), these values obviously decreased with increasing $f_B$ because of the change in either their microstructures or their water contents.

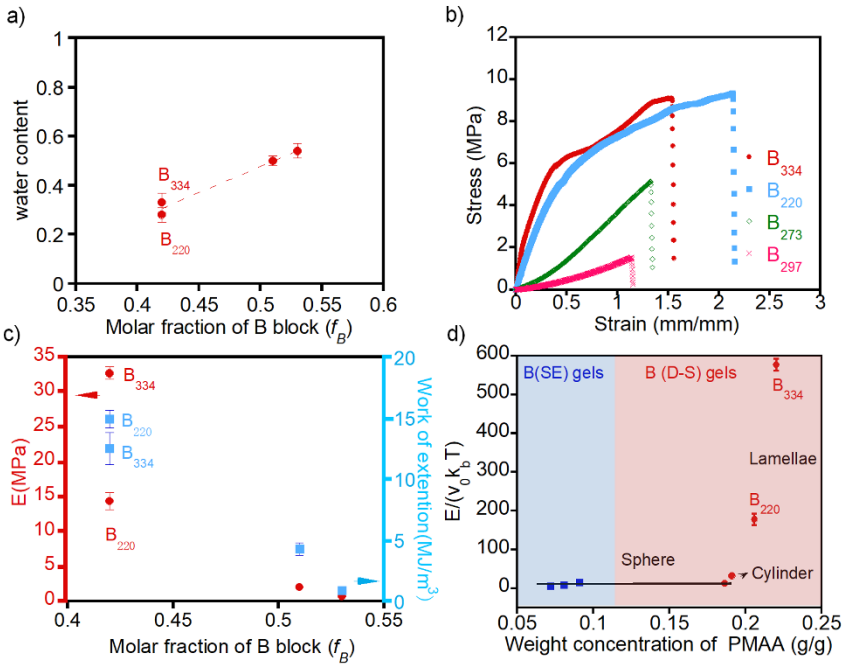


**Figure 3** a) Water content of the B(D-S) gels with different molar fraction of the B block ($f_B$) in ABA block copolymers; b) Tensile stress-strain curves of different B(D-S) gels; c) the modulus (E) and work of extension of the B(D-S) gels plotted as a function of the molar fraction of the B block in ABA block copolymers; d) Reduced modulus, $E/v_{mid}k_BT$, of B(SE) gels and B(D-S) gels as a function of the weight concentration of the B-block in the gel.

To identify the origin of the mechanical property change of the B(D-S) hydrogels, their reduced modulus was analyzed.[22] If the end-block domains in the tri-block copolymer gels are simply considered as crosslink points, the mechanical responses of

the tri-block copolymer gels can be described by the rubber elasticity theory,[22,25] which dictates the Young's modulus of an elastomeric gel consisting of Gaussian chains as follows:

$$E = 3vk_BTf$$

where $v$ is the number density of elastically active chains, $k_B$ is Boltzmann's constant, $T$ is the absolute temperature, and $f$ is the fraction of elastically effective chains.[27] In this study, the number density of mid-block chains $v_{mid}$ was estimated from the water concentration of the gels (Supporting information), and entanglement of the B-block chains were not taken into consideration. The reduced moduli, $E/v_{mid}k_BT$, of the B(D-S) hydrogels were plotted as a function of the weight concentration of the PMAA block (B block) in the hydrogels, as shown in Figure 3d. Data for the B(SE) hydrogels prepared from $B_{220}$, $B_{273}$, and $B_{297}$ tri-block copolymers were also plotted for comparison. The $E/v_{mid}k_BT$ of the B(SE) hydrogels and B(D-S) hydrogels with spherical structures had values of 5–10, which were slightly larger than the predicted value of 3. Possible reasons for this deviation include: 1) entanglements of B-block chains, which should exist but were not considered when calculating $v_{mid}$; 2) stretching of the mid-block chains, which leads to deviation in the elastic energy of each chain from $k_BT$. On the other hand, the $E/v_{mid}k_BT$ obviously increased for the B(D-S) hydrogel with a cylindrical structure and showed an even sharper increase for that with a lamellar structure. It means that TBC gels with cylinder or lamellae structure cannot be deemed as simple rubber-elastic materials as their large and anisotropic A

blocks also contribute to elasticity of the gels. Among the laminar B(D-S) hydrogels, the $B_{334}$(D-S) hydrogel showed a higher elastic modulus compared to the $B_{220}$(D-S) hydrogel. This may be because the longer hydrophobic chains of $B_{334}$ formed a thicker A domain (34.2 nm) than those of $B_{220}$ (20.4 nm). These results indicate that the elastic modulus of the B(D-S) hydrogels was not only determined by the rubber elasticity of the B-block chains but also highly affected by the micro-structured A-block. . Particularly, for laminar B(D-S) hydrogels, the rigid, planer A-phase contributes to mechanical robustness. The $B_{334}$(D-S) hydrogel containing ~30 wt% of water showed an elastic modulus of 32 MPa, fracture strain of 1.5, and fracture stress of 9 MPa, which is comparable to the mechanical strength of cartilage and skin.[28,29]

Although the obtained B(D-S) hydrogels with tunable modulus are relatively strong, they remain mechanically brittle, showing a fracture strain of less than 2. Thus, the linear PAAm chains, which can form sacrificial hydrogen bonds with the PMAA B-block of the TBCs, were introduced to the B(D-S) gels to enhance their mechanical performance.[25, 26] As the obtained semi-IPN hydrogels, named as B(D-S)/PAAm DN gels, showed no obvious swelling during or after introduction of the PAAm chains (Figure S5), the microstructures of the B(D-S) mother gels were considered to be preserved in the B(D-S)/PAAm DN gels. The S-S curves of B(D-S)/PAAm DN gels compared to those of the mother B(D-S) gels are shown in Figure 4. Introduction of PAAm into the B(D-S) gels effectively improved their fracture strain to ~4 and the

fracture stress to 8–12 MPa. Such improvements are originated from the PAAm-PMAA hydrogen bonding as sacrificial bonds, as discussed in our previous paper[26]. On the other hand, each B(D-S)/PAAm DN gel inherited the modulus of its mother B(D-S) gel, and the higher the modulus of the mother gel is, the higher the fracture stress of the B(D-S)/PAAm DN gel becomes. It suggests that the microstructure of A-block also contributes to the stiffness and stress of the B(D-S)/PAAm DN gels. In this way, we fabricated a series of TBC gels commonly showing high mechanical robustness to ensure high durability and with a controllable modulus of 1–20 MPa, expanding their potential applications. For laminar B(D-S) gels, the modulus slightly decreased after addition of PAAm. This may be because the introduced PAAm chains slightly interpenetrated the hydrophobic phase, which affected the stiffness of the hydrophobic laminar phase. This was also reflected in the slight change in size and water content of the gels after forming the B(D-S)/PAAm DN gels, as shown in Figure S6.

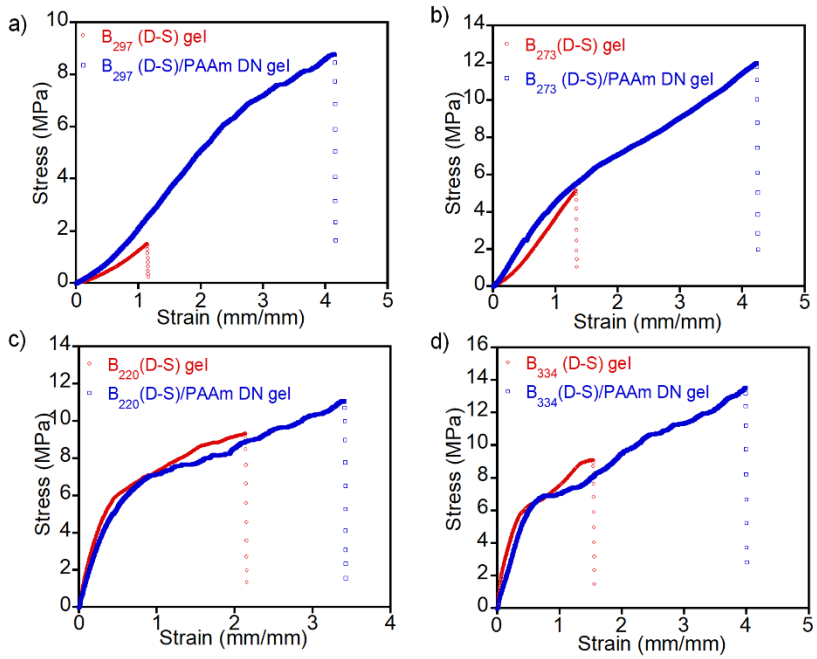


**Figure 4** Tensile stress-strain curves of B(D-S)/PAAm DN gels and corresponding mother B(D-S) gels based on different PBMA-b-PMAA-b-PBMA block copolymers: a) $B_{297}$, b) $B_{273}$, c) $B_{220}$, and d) $B_{334}$.

Microstructure of the TBC gels controls not only their mechanical properties but also their structure-related functions. Hydrogels with laminar structure are known to work as photonic gels with color responsibility to physical and chemical conditions, and they are potentially applicable as sensory or telecommunication devices.[9, 30] Here, we show that the B(D-S) gels with lamellar structure also work as environment-responsive photonic gels. As the TBCs in this study contain PMAA B-block, which is weak acid with pKa of 4.8, the B-block in the B(D-S) gels was expected to be swollen more at base condition, which induce red shift of light reflection spectrum of the gels. The light reflection spectra and corresponding photographs of the $B_{334}$(D-S) hydrogel at pH 8, 9,

10 and 14 are shown in figure 5a. It was found that the $B_{334}$(D-S) gel, which is colorless at low pH, became purple at pH 8−14 and showed the brightest structural color at pH 10 with the peak reflection wavelength of approx. 400 nm. The structural color in visible light range suggests the large (~100 nm scale) interlayer distances of the $B_{334}$(D-S) gel (figure 5b). The pH-dependent change of the interlayer distance is mainly originated form the preferential swelling of the $B_{334}$(D-S) gel along the thickness direction at base condition (Figure S7). The change of interlayer distance, however, was larger than that of gel thickness because the lamellar layers are not well aligned along the thickness direction, which is consistent with the SAXS measurement (figure 2d).

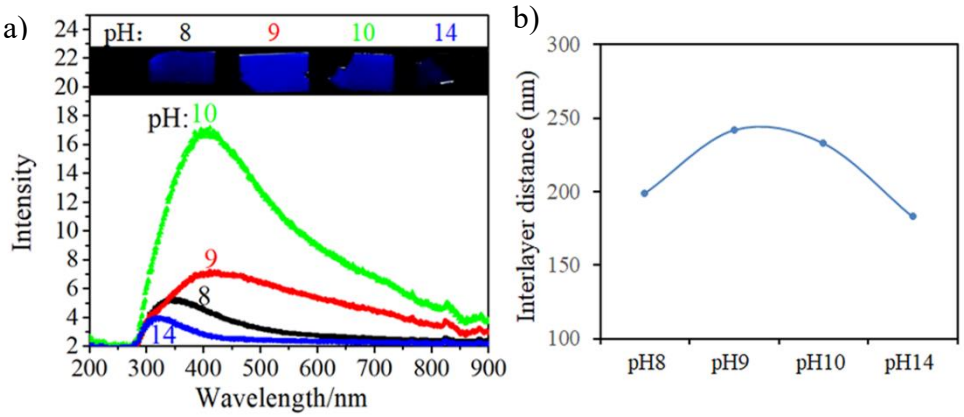


**Figure 5** a) The reflection spectra and corresponding photographs of the $B_{334}$(D-S) gel at different pH values, b) the interlayer distances of the $B_{334}$(D-S) gels calculated from the peak reflection wavelength.

In conclusion, we developed a simple drying-swelling method to construct tri-block copolymer hydrogels with different microstructures without changing the chemical

species of the monomeric units. Microstructures of the B(D-S) gels strongly affected their mechanical performance; particularly, the laminar structure greatly increased the modulus. By introducing PAAm as a second component to the B(D-S) gels, the TBC hydrogels with different microstructures became mechanically robust with sufficient stretchability of ~400% and high fracture stress of ~10 MPa, giving the gel greater application potential. Given the non-cytotoxicity of the B-DN hydrogels as well as their toughness, the B(D-S)/DN hydrogels might be suitable as modulus-tunable medical materials for artificial cartilage or artificial skin[25-26]. In addition to mechanical properties, the lamellar $B_{334}$(D-S) hydrogel became pH-sensitive photonic gel, which provide the gels potentially applicable as sensory devices.

Associated Content:

**Supporting information.** Materials, synthesis processes of all the gels, characterization methods, supplementary data, and calculated data.(PDF)

ACKNOWLEDGMENTS

This research was supported by JSPS KAKENHI (Grant Numbers JP17H04891 and JP17H06144) and ImPACT Program of Council for Science, Technology and Innovation (Cabinet Office, Government of Japan). The Institute for Chemical Reaction

Design and Discovery (ICReDD) was established by the World Premier International Research Initiative (WPI), MEXT, Japan. The authors thank Mr. Osamu Ito and Mr. Hiroyuki Ishitobi (Otsuka Chemicals) for providing tri-block copolymers.

References:

[1] Weiner, S; Traub, W; Wagner, H. D. Lamellar bone: structure–function relations. J Struct Bio. 1999, 126, 241−255.

[2] Sun, J; Bhushan., B. Hierarchical structure and mechanical properties of nacre: a review. RSC Advances 2012, 2, 7617−7632.

[3] Fung, Y. C. In Biomechanics: Mechanical properties of living tissues, 2nd ed.; Springer-Verlag Inc.: New York, 1993, p 392.

[4] Yasuda, K.; Kitamura, N.; Gong, J. P.; Arakaki, K.; Kwon, H. J.; Onodera, S.; Chen, Y. M.; Kurokawa, T.; Kanaya, F.; Ohmiya, Y.; Osada, Y. A novel double-network hydrogel induces spontaneous articular cartilage regeneration in vivo in a large osteochondral defect. Macromol Biosci. 2009, 9, 307−316.

[5] Senturk, B.; Macias, C. E.; Kung, J. H.; Muratoglu, O. K. Poly(vinyl alcohol)–acrylamide hydrogels as load-bearing cartilage substitute. H Biomater. 2009, 30, 589–596.

[6] Nonoyama, T.; Wada, S.; Kiyama, R.; Kitamura, N.; Mredha, Md. T. I.; Zhang, X.; Kurokawa, T.; Nakajima, T.; Takagi, Y.; Yasuda, K.; Gong, J. P. Anisotropic tough double network hydrogel from fish collagen and its spontaneous in vivo bonding to bone. Adv Mater. 2016, 28, 6740–6745.

[7] Gao, Y.; Zhao, F.; Wang, Q.; Zhang, Y.; Xu, B. Small peptide nanofibers as the matrices of molecular hydrogels for mimicking enzymes and enhancing the activity of enzymes. Chem Soc Rev. 2010, 39, 3425–3433.

[8] Mredha, T. I.; Guo, Y. Z.; Nonoyama, T.; Nakajima, T.; Kurokawa, T.; Gong, J. P. A facile method to fabricate anisotropic hydrogels with perfectly aligned hierarchical fibrous structures. Adv Mater. 2018, 30, 1704937.

[9] Yue, Y. F.; Haque, M. A.; Kurokawa, T.; Nakajima, T.; Gong, J. P. Lamellar hydrogels with high toughness and ternary tunable photonic stop-band. Adv Mater. 2013, 25, 3106–3110.

[10] Liu, M.; Ishida, Y.; Ebina, Y.; Sasaki, T.; Hikima, T.; Takata, M.; Aida, T. An anisotropic hydrogel with electrostatic repulsion between cofacially aligned nanosheets. Nature 2015, 517, 68–72.

[11] Matsen, M. W.; Thompson, R. B. Equilibrium behavior of symmetric ABA triblock copolymer melts. J Chem Phys. 1999, 111, 7139–7146.

[12] Mai, Y.; Eisenberg, A. Self-assembly of block copolymers. Chem Soc Rev. 2012, 41, 5969–5985.

[13] Lee, K.; Kobayashi, S. Polymer Materials: Block-Copolymers, Nanocomposites, Organic/Inorganic Hybrids, Polymethylenes. Springer, 2010, p 79.

[14] Hamiey, I. W. The physics of block copolymers, Oxford University Press, 1998, p 24.

[15] McKenzie, B. E.; Visser, J. F.; Friedrich, H.; Wirix, M. J. M.; Bomans, P. H. H.; With, G.; Holder, S. J.; Sommerdijk, N. A. J. M. Bicontinuous nanospheres from simple amorphous amphiphilic diblock copolymers. Macromolecules 2013, 46, 9845–9848.

[16] Koo, K.; Ahn, H.; Kim, S.; Ryu, D. Y.; Russell, T. P. Directed self-assembly of block copolymers in the extreme: guiding microdomains from the small to the large. Soft Matter 2013, 9, 9059–9071.

[17] Seitz, M. E.; Martina, D.; Baumberger, T.; Krishnan, V. R.; Hui, C.; Shull, K. R. Fracture and large strain behavior of self-assembled triblock copolymer gels. Soft Matter 2009, 5, 447–456.

[18] Guvendiren, M.; Shull. K. R. Self-assembly of acrylic triblock hydrogels by vapor-phase solvent exchange. Soft Matter 2007, 3, 619–626.

[19] Flanigan, C. M.; Crosby, A. J.; Shull, K. R. Structural development and adhesion of acrylic ABA triblock copolymer gels. Macromolecules 1999, 32, 7251–7262.

[20] Madsen, J.; Armes, S. P. (Meth) acrylic stimulus-responsive block copolymer hydrogels. Soft Matter 2012, 8, 592–605.

[21] Chantawansri, T. L.; Sirk, T. W.; Sliozberg, Y. R. Entangled triblock copolymer gel: Morphological and mechanical properties. J Chem Phys. 2013, 138, 024908.

[22] Seitz, M. E.; Burghardt, W.R.; Shull, K.R. Micelle morphology and mechanical response of triblock gels. Macromolecules 2009, 42, 9133–9140.

[23] Gong, J. P. Why are double network hydrogels so tough. Soft Matter 2010, 6, 2583-2590

[24] Henderson, K. J.; Zhou, T. C.; Otim, K. J.; Shull, K. R. Ionically cross-linked triblock copolymer hydrogels with high strength. Macromolecules 2010, 43, 6193–6201.

[25] Zhang, H. J.; Sun, T. L.; Zhang, A. K.; Ikura, Y; Nakajima, T.; Nonoyama, T.; Kurokawa, T.; Ito, O.; Ishitobi, H.; Gong, J. P. Tough physical double-network hydrogels based on amphiphilic triblock copolymers. Adv Mater. 2016, 28, 4884–4890.

[26] Ye, Y. N.; Frauenlob, M.; Wang, L.; Tsuda, M. ; Sun, T. L.; Cui, K.; Takahashi, R.; Zhang, H. J; Nakajima, T.; Nonoyama, T.; Kurokawa, T.; Tanaka, S.; Gong, J. P. Tough and self-recoverable thin hydrogel membranes for biological Applications. Adv Funct Mater. 2018, 1801489.

[27] Gent, A. N. Engineering with Rubber. 3rd ed. Hanser Publishers, Munich, 2012, p 40.

[28] Wegst, U. G. K.; Ashby, M. F. The mechanical efficiency of natural materials. Philosoph Mag. 2004, 84, 2167–2181.

[29] Bauer, A. M.; Russell, A. P.; Shadwick, R. E. Mechanical properties and morphological correlates of fragile skin in gekkonid lizards. J Exp Biol. 1989, 145, 79–102.

[30] Kang, Y.; Walish, J. J.; Gorishnyy, T.; Thomas, E. L. Broad-wavelength-range chemically tunable block-copolymer photonic gels. Nat mater. 2007, 6, 957-060